Published in final edited form as:
J Magn Reson Imaging. 2014 February ; 39(2): 377–386. doi:10.1002/jmri.24150.

Vessel-encoded arterial spin labeling (VE-ASL) reveals elevated flow territory asymmetry in older adults with substandard verbal memory performance

Manus J. Donahue, PhD[1,2,3,4,5,*], **Erin Hussey, PhD**[4], **Swati Rane, PhD**[1,2], **Tracy Wilson, MS**[1], **Matthias van Osch, PhD**[6], **Nolan Hartkamp, MD**[7], **Jeroen Hendrikse, MD, PhD**[7], and **Brandon A. Ally, PhD**[3,4]

[1]Vanderbilt University Institute of Imaging Science, Nashville, TN, USA

[2]Radiology and Radiological Sciences, Vanderbilt University, Nashville, TN, USA

[3]Psychiatry, Vanderbilt University School of Medicine, Nashville, TN, USA

[4]Neurology, Vanderbilt School of Medicine, Nashville, TN, USA

[5]Physics and Astronomy, Vanderbilt University, Nashville, TN, USA

[6]Radiology, Leiden University, Albinusdreef 2, 2333ZA, Leiden, NL

[7]Radiology, University Medical Center Utrecht, PO Box 85500, 3508 GA Utrecht, NL

Abstract

Purpose—To evaluate how flow-territory asymmetry and/or the distribution of blood through collateral pathways may adversely affect the brain's ability to respond to age-related changes in brain function. These patterns have been investigated in cerebrovascular disease, however here we evaluated how flow-territory asymmetry related to memory generally in older adults.

Materials and Methods—A multi-faceted MRI protocol, including vessel-encoded arterial spin labeling capable of flow territory mapping, was applied to assess how flow territory asymmetry; memory performance (CERAD-Immediate Recall); cortical cerebral blood flow (CBF), white matter lesion (WML) count, and cortical gray matter volume were related in older healthy control volunteers (HC; n=15; age=64.5±7 yrs) and age-matched mild cognitive impairment volunteers (MCI; n=7; age=62.7±3.7 yrs).

Results—An inverse relationship was found between memory performance and flow territory asymmetry in HC volunteers (P=0.04), which reversed in MCI volunteers (P=0.04). No relationship was found between memory performance and cortical tissue volume in either group (P>0.05). Group-level differences for HC volunteers performing above vs. below average on CERAD-I were observed for flow-territory asymmetry (P<0.02) and cortical volume (P<0.05) only.

Conclusion—Findings suggest that flow-territory asymmetry may correlate more sensitively with memory performance than CBF, atrophy and WML count in older adults.

Keywords

cerebral blood flow; memory; dementia; ageing; vessel encoded arterial spin labeling (VE-ASL); flow territory asymmetry

[*]**Corresponding Author:** Manus J. Donahue, 1161 21st Avenue South, AA 1105 MCN, Nashville, Tennessee, 37232-2310, Fax: 615-936-7247, Tel: 615-322-8350, mj.donahue@vanderbilt.edu.

Introduction

Both healthy ageing and age-related pathology have been associated with neurovascular impairment, however the specific impact of vascular changes on disease onset and progression remain highly controversial (1,2). Most prominently, vascular insufficiency is the causative focus of cerebrovascular disease (3), however similar vascular or hemodynamic abnormalities have also been associated (either in a primary or secondary role) with other neurological conditions, such as Parkinson's disease (4,5), epilepsy (6,7), Alzheimer's disease (8–10), and multiple sclerosis, (11,12). Yet, there is considerable debate regarding the role that vascular dynamics impose on aging and neurological disease, and to what extent observed aberrations are a cause, or a consequence, of disease.

More specifically, cerebral blood flow (CBF; ml blood/100g tissue/min) is an important physiological parameter, which has been extensively studied, and sensitively influences tissue homeostasis and the cerebral metabolic rate of glucose and oxygen consumption (3,13–15). As such, in scenarios of reduced cerebral perfusion pressure (CPP), extensive collateralization pathways are in place to maintain CBF (16). Thus, a measurement of the flow territory asymmetry, which may reflect the extent of collateralization, and in turn how capable the cerebrovasculature is to responding to future metabolic or hemodynamic inefficiency (17), and/or capable of clearing byproducts of metabolism, may be a more sensitive predictor of the rate of future cognitive decline than CBF alone.

Intracranial collateralization manifests both in terms of primary collaterals, as in the feeding arterial vessels of the circle of Willis (cW), and secondary collaterals, as in leptomeningeal vessels that may develop after acute or chronic ischemia (18). Importantly, a complete cW is prevalent in less than half of the population, and incomplete variants (e.g., absent or hypoplastic segments) influence both flow territory patterns and the ability of leptomeningeal vessels to develop (17). These variations may directly impact the brain's ability to compensate for metabolic changes associated with neurological disease mechanisms. Specifically, a reduction in the number of small and medium deep white matter lesions has been observed in volunteers with atherosclerotic disease who also possessed a fetal-type cW configuration (19). These data are in relative contrast to other studies suggesting that individuals with a complete cW may be better suited to respond to neurological events (18,20). Therefore, it is unclear how flow territory asymmetry may influence the neurobiology of aging.

This study aims to investigate the relationship between flow territory asymmetry and memory, one of the most basic cognitive phenomena altered in both healthy ageing and age-related pathology (21). Furthermore, both subcortical and cortical CBF and metabolism are implicated in memory dysfunction (22). We sought to understand to what extent flow territory asymmetry is related to memory performance, as well as to other more common imaging biomarkers of impairment such as cortical volume, cortical CBF, and white matter lesion (WML) count.

Measurement of flow territory asymmetry at the tissue level is not possible with conventional angiographic approaches. Very recently, an extension of the noninvasive CBF-weighted arterial spin labeling (ASL) MRI approach, termed vessel-encoded arterial spin labeling (VE-ASL), was introduced to allow for assessment of such flow territory asymmetry (3,17,23,24). In this approach, blood water in different feeding vessels is separately labeled noninvasively using a combination of phase-cycled radiofrequency (RF) pulses, and perfusion maps are subsequently derived that provide information both on CBF, as well as the specific vessel feeding the tissue. This method has been successfully applied

in patients with cervical and intracranial ischemic steno-occlusive disease (3,25,26), however has not been applied to assess the relationship between flow territory asymmetry and memory performance in older adults more generally. Here, VE-ASL is applied as part of a multi-faceted experiment to assess how flow territory asymmetry; memory performance; cortical CBF; WML count; and cortical gray matter volume are related in older adults.

Materials and Methods

Volunteer Recruitment

Volunteers (n=22; age=64.0±4.8 yrs) with no history of cerebrovascular disease and varying degrees of cognitive ability and dementia risk provided informed, written consent in this HIPAA-compliant, Institutional Review Board (IRB)-approved study. Volunteers with no clinical diagnosis of dementia (n=15; 64.5±7 yrs) were the primary focus of this study, and were considered separately from volunteers with single- or multi-domain amnestic MCI (n=7; age=62.7±3.7 yrs). Healthy volunteers were recruited without discrimination for sex through institutional flyers, whereas consecutive single or multi-domain amnestic MCI patients were referred consecutively, without discrimination for sex, from a neurology clinic between 1 February 2011 and 29 February 2012. MCI diagnosis was made by an experienced neurologist, using neuropsychological testing, MRI, and clinical interview.

Memory Testing

Each volunteer underwent a neurocognitive battery including the Mini-mental State Exam (MMSE) (27) and Consortium to Establish a Registry for Alzheimer's Disease (CERAD) Immediate (CERAD-I), Delay (CERAD-D) and Recognition (CERAD-R) exams (28). Higher performance on the CERAD exam indicates better memory, with a maximum score of 30 (CERAD-I) or 10 (CERAD-D and CERAD-R); encoding (CERAD-I) and retrieval (CERAD-D) rely on an intact cortical interaction between prefrontal regions and hippocampus. The ability to discriminate between studied and unstudied items (CERAD-R) relies on intact hippocampal functioning. Although there are a number of memory measures to chose from, the CERAD was used because it is known to provide a large range of scores, even in volunteers with clinically normal memory performance, and it is not confounded by other cognitive domains such as executive functioning or semantic categorization strategies (e.g., California Verbal Learning Test).

Genetic and Familial Risk Assessment

Information regarding dementia risk was obtained in terms of family history and genetic predisposition. Volunteers were considered "at-risk" if they possessed either one parent with Alzheimer's disease and/or at least one copy of the Apolipoprotein E (APOE)-ε4 allele. For genetic sequencing, a saliva sample was taken using an Oragene DNA kit (DNA Genotek Inc., Ontario, Canada) and processed at the Vanderbilt Center for Human Genetics using assays to discriminate between carriers for APOE-ε2, -ε3 and -ε4. Of the healthy volunteers (non-MCI), eight were controls and seven were at-risk. Note that the high number of at-risk subjects (approximately half of total volunteers) leads to a higher-than-average anticipated prevalence of APOE-ε4 in this sample.

MRI

All volunteers were scanned at 3.0T (Philips Medical Systems, Best, The Netherlands) using T_1-weighted and T_2-weighted FLuid Attenuated Inversion Recovery (FLAIR) structural, and VE-ASL MRI at 3.0T using body coil RF transmission and SENSE 8-channel reception. The VE-ASL method used in this study is very similar to a method recently validated and successfully used clinically to assess flow asymmetry in patients with cerebrovascular

disease (15,29). *Scan parameters.* VE-ASL: pseudo-continuous ASL (pCASL) labeling (1650 ms Hanning pulse train), post-labeling delay = 1650 ms, labeling offset = 90 mm, slices=15, spatial resolution = 3.5×3.5×7 mm, SENSE-factor=2.5, TE/TR=17/4000 ms. Labeling was performed separately for left ICA (LICA), right ICA (RICA) and vertebrobasilar arteries (VBA), yielding three separate flow territories (Figure 1). This was achieved in an automated fashion by performing five separate labeling scenarios: (i) no labeling (control), (ii) non-selective labeling of all feeding vessels at the location of the labeling plane (inter-pulse gradients off), (iii) varying inversion efficiency by 25 mm in R/L direction (LICA vs. RICA labeling), as well as (iv) 9 mm in anterior/posterior (A/P) direction and (v) 9 mm in A/P direction shifted by 4.5 mm (VBA labeling). The robustness and reproducibility of this methods has recently been reported (29). 3D T_1-weighted (MPRAGE: 1×1×1 mm^3; TR/TE=8.9/4.6 ms) and 2D (axial) T_2-weighted FLAIR (0.9×0.9×1 mm^3; TR/TE=11000/120 ms) images were acquired for cortical volumetric and white matter lesion quantification, respectively.

Analysis and Statistical Considerations

VE-ASL data were corrected for motion and baseline drift (30) and a k-means clustering algorithm (29), including a SNR threshold = 2.0, was used to group the different labeling geometries into three perfusion territories: flow from LICA, RICA, and VBA (Figure 1). Subsequently, VE-ASL data were registered (using the unlabeled gradient echo image as a template) to a 2 mm Montreal Neurological Institute (MNI) atlas using standard linear affine registration routines (30). The co-registered VE-ASL data were used to calculate the mean territory map of all volunteers to understand the spatial extent of the average flow territories. A common gray matter mask, defined from the Jülich histological atlas (31), was applied to ensure that exactly the same number of total cortical voxels were considered for each volunteer. This eliminated any bias from head size influencing the inter-subject flow asymmetry comparisons. Next, flow asymmetry was calculated for each volunteer, which was defined as how many flow territory voxels for each subject fell outside the mean flow territory map. This was performed separately for each of the three flow territories and the total voxel count is reported here as the flow asymmetry measure. Additionally, the number of perfusion voxels attributed to labeling of VBA, RICA, or LICA were calculated for all volunteers to obtain a probability index that a given voxel's perfusion was derived from a given feeding artery.

For cortical gray matter volume calculations, FreeSurfer (Athinoula A. Martinos Center, Boston, MA, USA) was applied to the T_1-weighted MPRAGE data and the calculated cortical gray matter volume was normalized by the intracranial volume (ICV) on a subject-by-subject basis (32). CBF in absolute units (ml/100g/min) was also quantified for each subject within the cortical mask through application of the solution to the single-compartment flow-modified Bloch equation to the ASL scenario where all inflowing blood water was labeled. We additionally calculated the CBF from each subject's flow territory mask, which was performed separately for VBA, RICA, and LICA flow territories in the subject's native space. Finally, total white matter lesion (WML) count was recorded from the FLAIR data, which was quantified visually by a neuroradiologist.

The primary statistical objective of this study was to assess the correlation between memory performance, as measured by the CERAD-I Word List Test, and the study covariate, i.e., flow territory asymmetry as calculated from the flow asymmetry value as defined above. A contingency aim was to determine whether flow territory asymmetry additionally reflects changes in cortical tissue volume, and whether the above trends are similar, or distinct, in older cognitively normal volunteers versus those with MCI. Descriptive statistics, including means, standard deviations, and ranges for continuous parameters, as well as percent and

frequency for categorical parameters, were evaluated. The non-parametric Spearman rank correlation coefficient (r_S) and corresponding p-value was calculated to test the above hypotheses, with the requirement $P < 0.05$ for significance. For group comparisons, an unpaired Student's t-test accounting for unequal variances was used with the requirement $P < 0.05$ for significance.

Results

Table 1 shows demographic, neuropsychological, flow asymmetry, structural volumes, perfusion values in each flow territory, and total WML count for all volunteers. No statistical group differences ($P > 0.05$) were observed between the control and at-risk populations when age, cognitive performance (as measured from the neuropsychological battery), flow asymmetry and cortical volume normalized by ICV were considered. As expected, MCI volunteers had reduced ($P < 0.01$) neuropsychological performance on average (MMSE=26.6±1.8; CERAD-I=13.9±4.3; CERAD-D=2.2±2.2; CERAD-R=6.6±3.6) relative to the non-MCI volunteers (MMSE=29.7±0.5; CERAD-I=21.3±4.0; CERAD-D=7.0±1.9; CERAD-R=9.8±0.6). Cortical volume was additionally reduced in MCI volunteers relative to non-MCI volunteers ($P < 0.01$). However, a large range of flow territory asymmetry was observed both within and between groups.

The primary goal of this study was to understand whether flow territory asymmetry correlated with memory performance in older individuals. Therefore, we compared the flow territory asymmetry values for the non-MCI volunteers with the CERAD-I score, which requires an intact interaction between cortical regions and hippocampus. This exam was the focus of this study as it is known to provide a large range of scores (Table 1; CERAD-I = 21.3 ± 4.0), even in volunteers with clinically normal memory performance. Figure 2A shows the average flow-territory maps across all volunteers, which demonstrate high symmetry between VBA (red), RICA (blue) and LICA (green) territories. Figure 2B shows representative slices from a volunteer with a high (good performer) CERAD-I score and corresponding normal symmetry in the flow territories. Figure 2C shows representative slices from a volunteer with a lower (CERAD=18) score, who shows higher asymmetry specifically in RICA and VBA territories (black arrow). The mean CERAD-I score for non-MCI volunteers was 21.3±4.0.

To better illustrate this effect, Figure 3 shows the probability that a given voxel derived flow from the VBA, RICA, or LICA, separately for the healthy volunteers with above average and below average memory performance. Increased flow territory asymmetry is observed in the poor performers compared to the good performers.

When volunteers were grouped as "high performers" (CERAD-I > average = 21) versus "low performers" (CERAD less than or equal to average = 21), a large distinction was observed ($P = 0.029$); discrepancy between cortical volumes was much less prominent between these two populations ($P = 0.089$) (Figure 4A,B). These findings lend support for flow territory asymmetry representing a more sensitive indicator of cognitive performance than cortical volume in older adults at risk for dementia. Furthermore, when volunteers were stratified as at-risk vs. control, no difference in flow territory asymmetry was observed. Figure 4C shows a trend for a reduction in cortical CBF between good performers, poor performers, and MCI volunteers, with a significant reduction in CBF being observed between the good performer and MCI groups only ($P<0.01$). Finally, a large variation in WMLs was observed in all volunteer groups, and no significant difference was observed between these groups for total WML count ($P>0.05$).

Figure 5 shows scatter plots of the cortical CBF in VBA, LICA and RICA flow territories for each volunteer. As can be seen, CBF values are tightly correlated ($P<0.01$) between the flow territories across all volunteers, demonstrating that while the degree of flow territory asymmetry does vary with memory performance, the CBF value (ml/100g/min) in the cortex is not particularly discrepant on average between flow territories.

Figure 6 shows scatter plots depicting the relationships between CERAD-I and flow territory asymmetry (Figure 6A), cortical volume / ICV and flow territory asymmetry (Figure 6B) and cortical volume / ICV and CERAD-I score (Figure 6C) in non-MCI volunteers. A significant anti-correlation is found between CERAD-I and flow territory asymmetry ($P = 0.04$) and cortical volume / ICV and flow territory asymmetry ($P=0.01$), yet only a weak trend for a relationship between cortical volume / ICV and CERAD-I is observed. This trend is largely driven by a single volunteer (Table 1; subject ID 14) who is discussed in the following section. A positive relationship between flow territory asymmetry and CERAD-I was found in the smaller cohort ($n=7$) of MCI volunteers ($r_s=0.70$; $P=0.04$).

Discussion

While VE-ASL has been applied recently to successfully assess collateral flow patterns in patients with cervical and intracranial ischemic steno-occlusive disease, to our knowledge these results demonstrate the first application of VE-ASL to study memory performance, and furthermore these results lend support for a relationship between flow territory asymmetry and memory in cognitively normal older adults.

Based on elevated flow territory asymmetry findings in the lower cognitive performers in the non-MCI group, we hypothesized that MCI volunteers would exhibit even more flow territory asymmetry secondary to more severe hemodynamic impairment. Interestingly, an opposite trend in the MCI volunteers was observed, indicating that the consequence of elevated flow territory asymmetry in older adults with clinical symptoms of dementia may differ from older healthy individuals at risk for dementia. This finding is not wholly surprising. For instance, the extent of intracranial vascular stenosis and the presence or absence of collaterals have traditionally been used as surrogates for disease severity and in particular cerebrovascular disease risk. However, it is unclear how arterial stenosis and/or pathological angiogenesis translates to parenchymal impairment at the tissue level. This question is fundamental, as large vessel disease and related flow territory asymmetry do not relate to hemodynamic compromise directly: in patients with intracranial stenosis, it has recently been demonstrated that collaterals may either reflect aggressive, unstable disease or alternatively adequate protective compensatory mechanisms (33). A similar occurrence could be present in patients with MCI. In other words, elevated flow territory asymmetry may be an early indicator of pathology in healthy older adults, however in patients with MCI flow territory asymmetry may evolve into a protective mechanism by providing additional hemodynamic resources to tissue operating at or near cerebrovascular reserve. These findings should provide motivation to pursue this topic in a larger study of patients with MCI and varying memory performance.

While the above hypothesis is speculative at this point, MRI holds promise for elucidating this relationship and providing an alternative diagnostic technique to digital subtraction angiography (DSA) for gauging the size and extent of collateral vessels, which is currently the gold standard for staging collateralization in steno-occlusive disease. Importantly, significant vascular risks and contrast-related complications hinder widespread use of DSA as a diagnostic tool in dementia patients. Experimentally, this work shows that a noninvasive VE-ASL approach can be applied successfully in dementia patients. Ongoing work is focused on using the proposed, and related hemodynamic, MRI approaches to longitudinally

track cognitive changes in older volunteers. Importantly, as these approaches are completely noninvasive and can be performed using standard MRI equipment available at most hospitals, they represent a promising avenue for studying sensitive functional biomarkers of dementia risk that may precede cognitive symptoms or irreversible tissue damage.

Furthermore, MRI allows for many measurements to be made in a single scan session. These measurements, such as tissue volume, white matter hyperintensities (FLAIR), cerebral microbleeds (susceptibility weighted imaging: SWI), and flow asymmetry (VE-ASL) may not be indicative of cognitive changes in isolation, but in combination may provide more telling information. This collective strategy has been employed here whereby genetic, neuropsychological, structural and functional information was combined to understand relationships between many of these measures. For instance, patient 14 (Table 1), does not meet the clinical criteria for MCI, yet some of his cognitive measures (e.g. CERAD-I and CERAD-D) border on what would be expected for an MCI patient. Interestingly, tissue volume is reduced and flow territory asymmetry elevated in this volunteer, which collectively provide additional support for a possible underlying pathological process. Future longitudinal studies, in conjunction with statistical prediction models, are required to confirm whether such metrics can be used collectively to better gauge older volunteers at-risk for accelerated cognitive decline.

It should also be noted that the purpose of this study was to investigate the presence of a relationship between flow territory asymmetry and memory performance in cortex. In an independent study using a very similar cohort (34), we investigated the relationship between subcortical perfusion and memory performance and observed that in cognitively normal older adults hippocampal perfusion correlated inversely with verbal memory performance. This finding is consistent with increasing data supporting unique hemodynamic compensatory phenomena in those at elevated risk for memory disorders (35,36).

The role that vascular changes have on dementia risk and trajectory are unclear. Epidemeological studies have demonstrated that non-steroidal anti-inflammatory drugs (NSAIDs) may reduce dementia risk, leading to the hypothesis that brain inflammation may be a significant contributing factor to memory disorders (37). However, drugs that lack anti-inflammatory activity have been demonstrated to reduce dementia risk (38), and furthermore glucocorticoid steroids, anti-inflammatory agents which regulate the transcription of chemokines and other inflammatory molecules, have been reported to have a much weaker effect on dementia treatment (39); thus, the mechanism by which neuroinflammation may mediate changes in memory function and progression are incompletely understood.

Importantly, vascular endothelial cells respond to neuroinflammation by secreting cytokine growth factors, which initiate angiogenesis to augment the existing cerebrovasculature to maintain energy requirements in tissue. It has further been hypothesized that angiogenic activation of vascular endothelium may lead to αβ deposition and corresponding neurotoxicity (38). Briefly, it has been observed that brain capillaries in older patients with severe memory disorders contain preamyloid deposits (40), which in turn generate reactive oxygen species that interact pathologically with vascular endothelium (41). This leads to intravascular accumulation of thrombin, a coagulation and angiogenic factor, which in turn activates a protein kinase C-dependent pathway whereby amyloid precursor protein (APP) is elicited. Increased levels of APP lead to further accumulation of αβ plaque, additional reactive oxygen species, thrombin accumulation, and correspondingly angiogenesis and APP. The above pathway supports the hypothesis that changes in memory performance may be partly linked to pathological angiogenesis manifested by increases in microvascular density (pathological angiogenesis) and intravascular plaque. The manner in which the brain compensates for such variations in blood flow likely also depends on the type of

redundancies in the cerebral circulation, such as the cW variant. Testing of this hypothesis is difficult, as detection of such neovascularization and corresponding collateralization is not possible at the spatial resolution afforded with conventional angiographic approaches and furthermore studies must be designed that target patients in very early or preclinical stages of disease. While the current study lacks the statistical power and longitudinal or cross-sectional component to support this hypothesis, it does provide evidence for flow territory asymmetry being elevated in older volunteers with below average verbal memory performance, which may motivate the need for larger studies of this type in a larger cohort.

Several limitations of the current study should be considered. First, the sample size was relatively small (n=22), however even with this small sample size we observed significant correlations between flow asymmetry and cognitive performance and more importantly these relationships were much stronger than those observed between cognitive performance and tissue volume. Owing to the smaller sample size, we deliberately avoided making claims regarding differences between the at-risk and control populations, however future studies which include a larger number of volunteers would be useful for identifying differences between these populations. Larger studies, especially in the MCI population, are anticipated to be useful for better understanding the role of collateralization as a protective versus pathological mechanism in these patients. Second, in addition to a possible mechanism of intravascular plaque leading to increased flow territory asymmetry, it is also anticipated that normal variants in the cW could account for much of the observed findings. Only about 40% of the population has a complete circle of Willis, and therefore it is anticipated that some of the variability in flow territory asymmetry could be accounted for by cW variants. Unfortunately, angiograms were not collected in these volunteers and therefore it is not possible to account for cW subtype from our data. It is possible that in older adults with varying hemodynamic compromise, the cW type may be protective, as has also been suggested in a separate study for volunteers with fetal type posterior variants (19). Third, the cognitive score that was the primary focus of this work (CERAD-I), is only one of many cognitive tests that could be performed, and like most tests broadly assesses memory performance. This test was selected for this study owing to its large range of values, even in cognitively normal volunteers. However, it is anticipated that other memory exams may provide different relationships with flow asymmetry, in both cortical and subcortical regions, and understanding such discrepancies is the topic of ongoing work. Fourth, we did not measure bolus arrival times by performing multiple inversion delay ASL measurements and therefore perfusion values in borderzone regions, where arterial arrival times may be longer (42,43), should be interpreted with caution. Owing to the relatively long labeling duration and post-labeling delay employed, combined with the very broad perfusion territories considered here, we do not believe this presents an overwhelming confound for the interpretation of these data. Finally, to enable comparison of maps across subjects, all volunteer data was co-registered to a standard 2 mm MNI atlas. This co-registration occurred after CBF calculation in the native space. The focus of this study was on broad flow territory patterns, however care should be taken in interpreting any flow changes on the scale below the nominal spatial resolution of 3.5×3.5×7 mm.

In conclusion, we measured changes in flow territory asymmetry using a recently reported and noninvasive vessel-encoded arterial spin labeling (VE-ASL) MRI approach. In cognitively normal older adults, it was observed that flow territory asymmetry was a more sensitive indicator of memory performance than structural tissue volume measurements (Figure 6). Furthermore, these relationships were found to diverge in a smaller cohort of MCI populations. These findings, combined with the noninvasive nature of the VE-ASL approach, suggest that detailed studies of flow territory asymmetry and related hemodynamic compensatory phenomena may report unique and useful information for portending cognitive decline in older adults and should be the focus of further investigation.

Acknowledgments

We are grateful to Dave Pennell, Leslie McIntosh, Donna Butler, and Chuck Nockowski for experimental support.

Grant Support:

Dr. Donahue is partly supported by a grant from the Vanderbilt Institute for Clinical and Translational Research. Additional support provided from: NIH/NINDS 1R01NS07882801A1.

References

1. Aanerud J, Borghammer P, Chakravarty MM, et al. Brain energy metabolism and blood flow differences in healthy aging. J Cereb Blood Flow Metab. 2012; 32(7):1177–1187. [PubMed: 22373642]
2. Kovacic JC, Moreno P, Nabel EG, Hachinski V, Fuster V. Cellular senescence, vascular disease, and aging: part 2 of a 2-part review: clinical vascular disease in the elderly. Circulation. 2011; 123(17):1900–1910. [PubMed: 21537006]
3. Donahue MJ, Strother MK, Hendrikse J. Novel MRI approaches for assessing cerebral hemodynamics in ischemic cerebrovascular disease. Stroke. 2012; 43(3):903–915. [PubMed: 22343644]
4. Rektor I, Goldemund D, Bednarik P, et al. Impairment of brain vessels may contribute to mortality in patients with Parkinson's disease. Mov Disor. 2012 [E-pub ahead of print].
5. Vokatch N, Grotzsch H, Mermillod B, Burkhard PR, Sztajzel R. Is cerebral autoregulation impaired in Parkinson's disease? A transcranial Doppler study. J Neurol Sci. 2007; 254(1–2):49–53. [PubMed: 17275849]
6. Sharma VK, Teoh HL, Chan BP. Cerebral vasomotor reactivity in epilepsy patients. J Neurol. 2010; 257(9):1565. [PubMed: 20339861]
7. Chen TH, Huang CC, Chang YY, Chen YF, Chen WH, Lai SL. Vasoconstriction as the etiology of hypercalcemia-induced seizures. Epilepsia. 2004; 45(5):551–554. [PubMed: 15101837]
8. de la Torre JC. Is Alzheimer's disease a neurodegenerative or a vascular disorder? Data, dogma, and dialectics. Lancet Neurol. 2004; 3(3):184–190. [PubMed: 14980533]
9. Yezhuvath US, Uh J, Cheng Y, et al. Forebrain-dominant deficit in cerebrovascular reactivity in Alzheimer's disease. Neurobiol Aging. 2012; 33(1):75–82. [PubMed: 20359779]
10. Filippini N, MacIntosh BJ, Hough MG, et al. Distinct patterns of brain activity in young carriers of the APOE-epsilon4 allele. Proc Natl Acad Sci U S A. 2009; 106(17):7209–7214. [PubMed: 19357304]
11. Fjeldstad AS, McDaniel J, Witman MA, et al. Vascular function and multiple sclerosis. J Neurol. 2011; 258(11):2036–2042. [PubMed: 21544565]
12. Singh AV, Zamboni P. Anomalous venous blood flow and iron deposition in multiple sclerosis. J Cereb Blood Flow Metab. 2009; 29(12):1867–1878. [PubMed: 19724286]
13. Raichle ME, Grubb RL Jr, Gado MH, Eichling JO, Ter-Pogossian MM. Correlation between regional cerebral blood flow and oxidative metabolism. In vivo studies in man. Arch Neurol. 1976; 33(8):523–526. [PubMed: 942309]
14. Grubb RL Jr, Raichle ME, Gado MH, Eichling JO, Hughes CP. Cerebral blood flow, oxygen utilization, and blood volume in dementia. Neurology. 1977; 27(10):905–910. [PubMed: 561903]
15. Donahue MJ, Ayad M, Moore R, et al. Relationships Between Hypercarbia Reactivity, Cerebral Blood Flow, and Arterial Circulation Times in Patients With Moyamoya Disease. J Magn Reson Imaging. 2013 [E-pub ahead of print].
16. Liebeskind DS. Collateral circulation. Stroke. 2003; 34(9):2279–2284. [PubMed: 12881609]
17. Hendrikse J, van der Grond J, Lu H, van Zijl PC, Golay X. Flow territory mapping of the cerebral arteries with regional perfusion MRI. Stroke. 2004; 35(4):882–887. [PubMed: 14988567]
18. van Raamt AF, Mali WP, van Laar PJ, van der Graaf Y. The fetal variant of the circle of Willis and its influence on the cerebral collateral circulation. Cerebrovasc Dis. 2006; 22(4):217–224. [PubMed: 16788293]

19. van der Grond J, van Raamt AF, van der Graaf Y, Mali WP, Bisschops RH. A fetal circle of Willis is associated with a decreased deep white matter lesion load. Neurology. 2004; 63(8):1452–1456. [PubMed: 15505164]
20. Van Overbeeke JJ, Hillen B, Tulleken CA. A comparative study of the circle of Willis in fetal and adult life. The configuration of the posterior bifurcation of the posterior communicating artery. J Anat. 1991; 176:45–54. [PubMed: 1917674]
21. Albert MS. The ageing brain: normal and abnormal memory. Philos Trans R Soc Lond B Biol Sci. 1997; 352(1362):1703–1709. [PubMed: 9415922]
22. Heiss WD, Pawlik G, Holthoff V, Kessler J, Szelies B. PET correlates of normal and impaired memory functions. Cerebrovasc Brain Metab Rev. 1992; 4(1):1–27. [PubMed: 1562450]
23. Wong EC, Cronin M, Wu WC, Inglis B, Frank LR, Liu TT. Velocity-selective arterial spin labeling. Magn Reson Med. 2006; 55(6):1334–1341. [PubMed: 16700025]
24. Helle M, Norris DG, Rufer S, Alfke K, Jansen O, van Osch MJ. Superselective pseudocontinuous arterial spin labeling. Magn Reson Med. 2010; 64(3):777–786. [PubMed: 20597127]
25. Hendrikse J, van der Zwan A, Ramos LM, et al. Altered flow territories after extracranial-intracranial bypass surgery. Neurosurgery. 2005; 57(3):486–494. discussion 486–494. [PubMed: 16145527]
26. Van Laar PJ, Hendrikse J, Mali WP, et al. Altered flow territories after carotid stenting and carotid endarterectomy. J Vasc Surg. 2007; 45(6):1155–1161. [PubMed: 17543680]
27. Bleecker ML, Bolla-Wilson K, Kawas C, Agnew J. Age-specific norms for the Mini-Mental State Exam. Neurology. 1988; 38(10):1565–1568. [PubMed: 3419600]
28. Morris JC, Mohs RC, Rogers H, Fillenbaum G, Heyman A. Consortium to establish a registry for Alzheimer's disease (CERAD) clinical and neuropsychological assessment of Alzheimer's disease. Psychopharmacol Bull. 1988; 24(4):641–652. [PubMed: 3249766]
29. Gevers S, Bokkers RP, Hendrikse J, et al. Robustness and reproducibility of flow territories defined by planning-free vessel-encoded pseudocontinuous arterial spin-labeling. AJNR Am J Neuroradiol. 2012; 33(2):E21–E25. [PubMed: 21393410]
30. Jenkinson M, Bannister P, Brady M, Smith S. Improved optimization for the robust and accurate linear registration and motion correction of brain images. Neuroimage. 2002; 17(2):825–841. [PubMed: 12377157]
31. Eickhoff SB, Stephan KE, Mohlberg H, et al. A new SPM toolbox for combining probabilistic cytoarchitectonic maps and functional imaging data. Neuroimage. 2005; 25(4):1325–1335. [PubMed: 15850749]
32. Fischl B, Dale AM. Measuring the thickness of the human cerebral cortex from magnetic resonance images. Proc Natl Acad Sci U S A. 2000; 97(20):11050–11055. [PubMed: 10984517]
33. Liebeskind DS, Cotsonis GA, Saver JL, et al. Collaterals dramatically alter stroke risk in intracranial atherosclerosis. Ann Neurol. 2011; 69(6):963–974. [PubMed: 21437932]
34. Rane S, Ally BA, Hussey E, et al. Inverse correspondence between hippocampal perfusion and verbal memory performance in older adults. Hippocampus. 2012
35. Filippini N, Ebmeier KP, MacIntosh BJ, et al. Differential effects of the APOE genotype on brain function across the lifespan. Neuroimage. 2011; 54(1):602–610. [PubMed: 20705142]
36. Quiroz YT, Budson AE, Celone K, et al. Hippocampal hyperactivation in presymptomatic familial Alzheimer's disease. Ann Neurol. 2010; 68(6):865–875. [PubMed: 21194156]
37. in t' Veld BA, Ruitenberg A, Hofman A, et al. Nonsteroidal antiinflammatory drugs and the risk of Alzheimer's disease. N Engl J Med. 2001; 345(21):1515–1521. [PubMed: 11794217]
38. Vagnucci AH Jr, Li WW. Alzheimer's disease and angiogenesis. Lancet. 2003; 361(9357):605–608. [PubMed: 12598159]
39. Gambassi G, Landi F, Bernabei R. Steroid therapy in AD. Neurology. 1997; 48(5):1473–1474. [PubMed: 9153504]
40. Miyakawa T. Electron microscopy of amyloid fibrils and microvessels. Ann N Y Acad Sci. 1997; 826:25–34. [PubMed: 9329678]
41. Liu F, Lau BH, Peng Q, Shah V. Pycnogenol protects vascular endothelial cells from beta-amyloid-induced injury. Biol Pharm Bull. 2000; 23(6):735–737. [PubMed: 10864026]

42. Chappell MA, MacIntosh BJ, Donahue MJ, Gunther M, Jezzard P, Woolrich MW. Separation of macrovascular signal in multi-inversion time arterial spin labelling MRI. Magn Reson Med. 2010; 63(5):1357–1365. [PubMed: 20432306]

43. MacIntosh BJ, Filippini N, Chappell MA, Woolrich MW, Mackay CE, Jezzard P. Assessment of arterial arrival times derived from multiple inversion time pulsed arterial spin labeling MRI. Magn Reson Med. 2010; 63(3):641–647. [PubMed: 20146233]

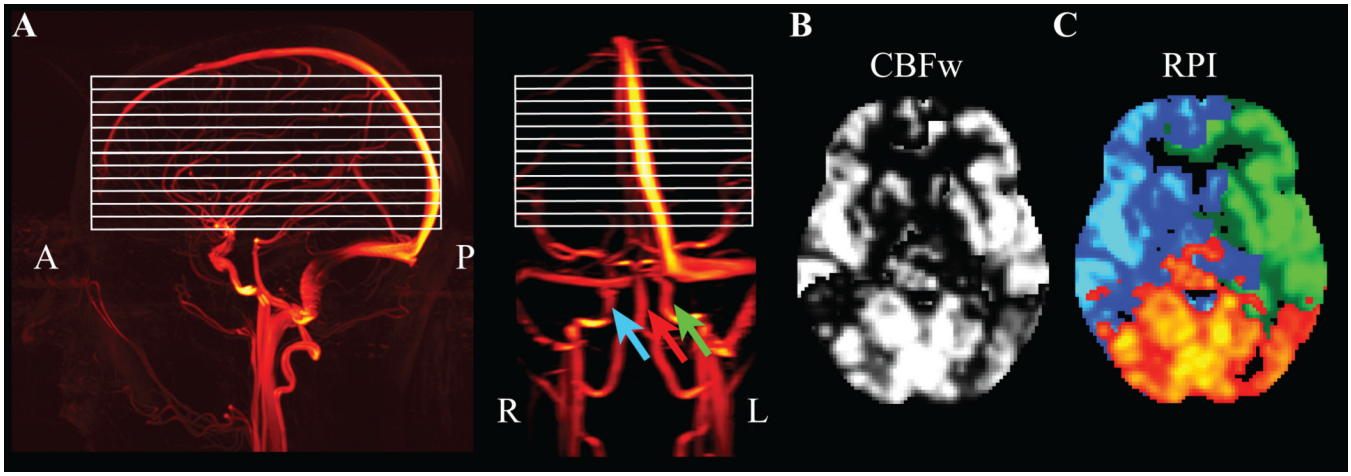

Figure 1.

Noninvasive regional perfusion imaging (RPI) using the vessel-encoded arterial spin labeling (VE-ASL) cerebral blood flow-weighted (CBFw) MRI approach. (A) Sagittal (left) and coronal (right) images from an MR angiography acquisition show the approximate region of slice placement (white); colored arrows demonstrate the locations of blood water labeling, separately for the left and right internal carotid artery (ICA; green, blue) and the basilar artery (red). (B) When blood water in all vessels is labeled simultaneously, a CBFw map is obtained. (C) However, when the different labeling conditions are considered separately, perfusion information from left ICA (blue), right ICA (green) and basilar artery (red) can be obtained, providing an indicator of flow territory asymmetry.

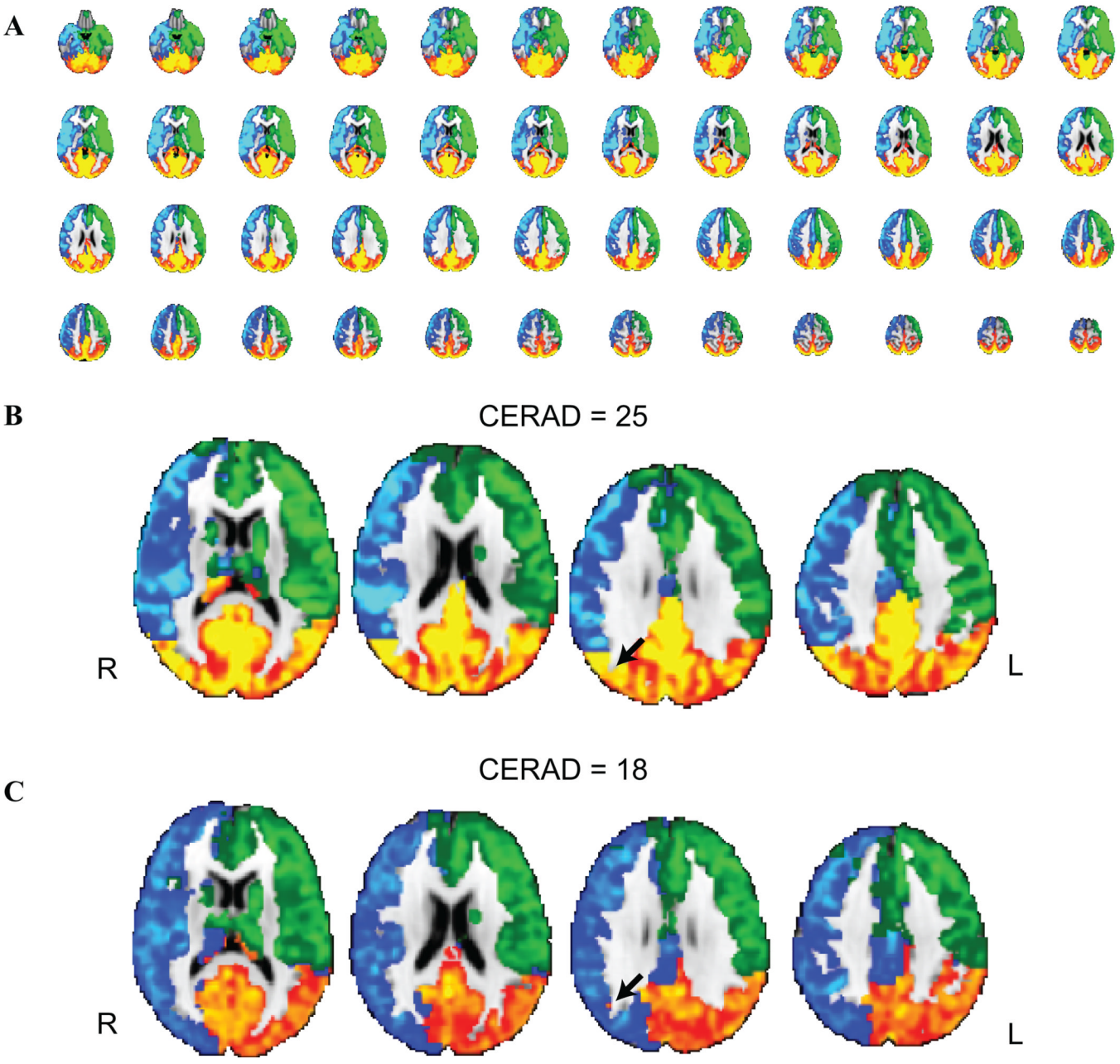

Figure 2.

Flow territory asymmetry classification using vessel-encoded arterial spin labeling (VE-ASL). (A) Group averaged (n=22) collateral flow maps from all volunteers depict relatively symmetric perfusion territories between right internal carotid artery (ICA) (blue), left ICA (green) and within vertebrobasilar (red) territories. (B) A subset of slices from a healthy volunteer who performed well on the Consortium to Establish a Registry for Alzheimer's Disease (CERAD) immediate recall test and (C) a separate healthy volunteer who performed below average. The volunteer in (C) shows increased flow territory heterogeneity, likely secondary to a fetal type circle of Willis (cW).

Figure 3.

Flow territory probability maps from healthy control volunteers who performed above average (left) vs. below average (right) on the memory task. The voxel intensity corresponds to the fraction of times (over all subjects) that the voxel received blood from the labeled vessel (VBA: vertebrobasilar artery; RICA: right internal carotid artery; LICA: left internal carotid artery). More variability is observed in the probability maps for the poor performers relative to the good performers. Color bar denotes fraction of volunteers with CBF derived from denoted vessel (e.g. 0 = 0% and 1 = 100%).

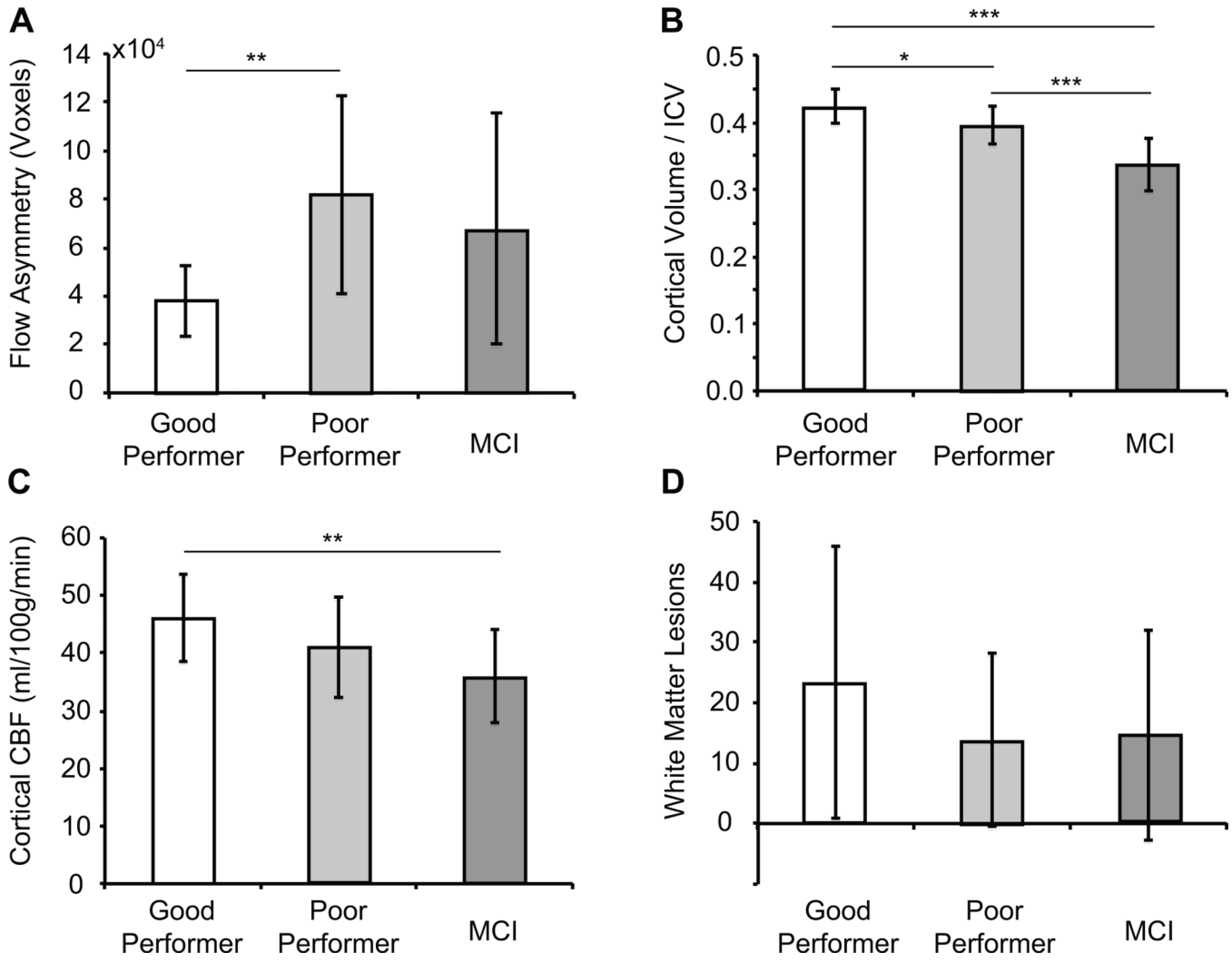

Figure 4.

Bar plots of group-level findings between different imaging measures. (A) When all healthy volunteers are considered (n = 15), the flow territory asymmetry is statistically elevated in lower performers (CERAD-I ≤ 21) relative to higher performers (CERAD-I > 21). No significant finding was observed in the MCI volunteers, suggesting that flow territory asymmetry may play a more complex or varied role in demented volunteers. (B) Cortical volume varied between groups in an expected manner. (C) A trend for a reduction in cortical CBF was found between good and poor performers, and (D) no difference in the total white matter lesion count was found between any of the groups. *** P<0.01; ** P<0.02; * P<0.05.

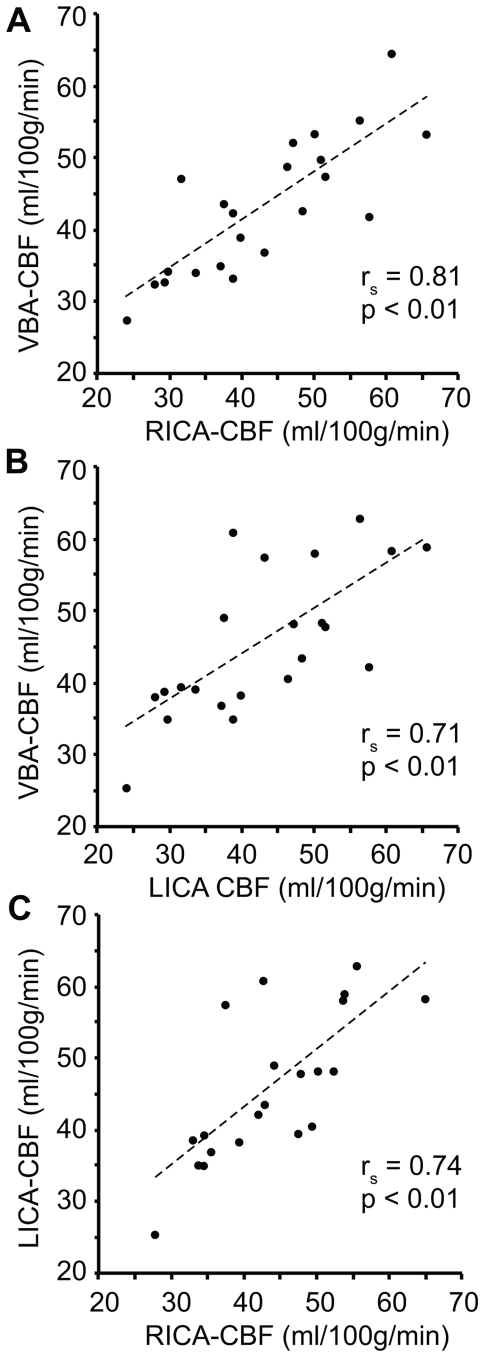

Figure 5.
Correlation plots between the cerebral blood flow (CBF) measured from different flow territories (VBA: vertebrobasilar artery; RICA: right internal carotid artery; LICA: left internal carotid artery) for all volunteers (n=22). These data demonstrate that on average CBF values are highly correlated between different flow territories, although the extent of each flow territory varies between volunteers (e.g., Figure 6). The Spearman rank correlation coefficient (r_S) and corresponding one-sided p-values are shown as well.

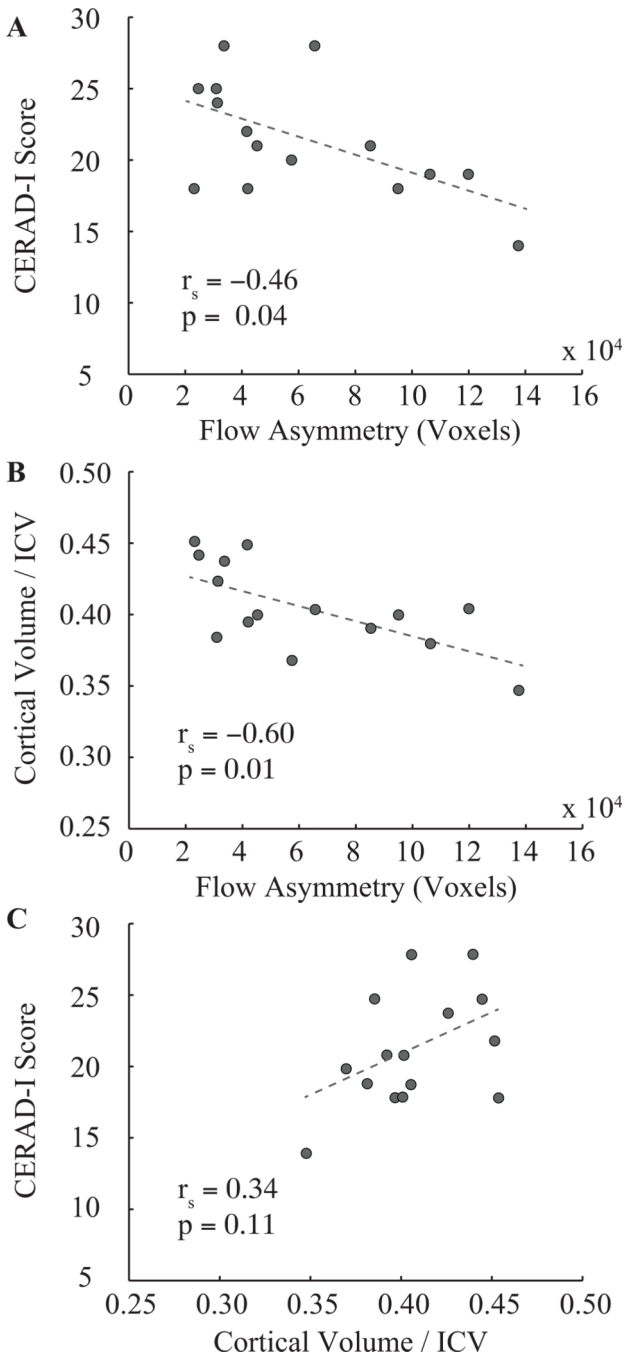

Figure 6.

Correlative findings between cognitive performance, flow territory asymmetry, and cortical volume in healthy older volunteers (n = 15). The Spearman rank correlation coefficient (r_s) and corresponding one-sided p-values are shown as well. Both cognitive performance (A) and cortical volume, normalized by intracranial volume: ICV (B), correlate inversely with flow asymmetry. (D) A weak trend for a correlation (P = 0.11) is found between cortical volume and cognitive performance.

Table 1

Volunteer demographics

Subject (Case)	Category	Sex	MMSE	CERAD-I	CERAD-D	CERAD-R	Flow Asymmetry (voxels)	Cortical Volume / ICV	VBA-CBF	RICA-CBF	LICA-CBF	WML
1 (6)	Control	F	30	22	9	10	41714	0.449	50	54	58	4
2 (8)	Control	F	30	28	10	10	65696	0.403	38	44	49	12
3 (10)	Control	F	30	25	9	10	30961	0.384	51	51	49	52
4 (11)	Control	F	30	19	8	10	119888	0.404	47	52	48	16
5 (12)	Control	M	30	18	4	9	95057	0.400	39	34	35	7
6 (13)	Control	F	29	24	10	10	31380	0.423	46	49	41	13
7 (20)	Control	F	30	28	6	10	33713	0.437	37	35	37	7
8 (24)	Control	M	29	19	5	10	106346	0.380	34	35	40	N/A
9 (7)	At-risk	F	29	21	8	10	85334	0.390	58	42	43	1
10 (17)	At-risk	F	30	18	6	8	23124	0.451	48	43	44	25
11 (21)	At-risk	F	29	20	6	10	57529	0.368	32	48	40	53
12 (22)	At-risk	F	30	25	7	10	24618	0.442	56	56	63	52
13 (25)	At-risk	F	30	21	6	10	45335	0.400	66	54	59	6
14 (9)	At-risk	M	29	14	5	10	137528	0.347	39	43	61	40
15 (19)	At-risk	M	30	18	6	10	42080	0.395	40	39	39	2
Mean			**29.7**	**21.3**	**7.0**	**9.8**	**62686**	**0.405**	**45.3**	**45.1**	**47.2**	**20.7**
STD			**0.5**	**4.0**	**1.9**	**0.6**	**37207**	**0.030**	**9.7**	**7.3**	**9.4**	**19.9**
16 (14)	MCI	F	27	13	2	8	75142	0.313	29	33	39	4
17 (15)	MCI	M	29	16	6	8	56283	0.363	30	34	35	6
18 (18)	MCI	M	27	20	4	10	168905	0.369	28	33	38	11
19 (23)	MCI	M	26	8	2	7	41574	0.360	24	28	26	1
20 (26)	MCI	M	27	17	0	2	66258	0.357	43	37	58	4
21 (27)	MCI	M	27	9	1	10	38206	0.260	61	65	59	45
22 (28)	MCI	F	23	14	0	1	27758	0.338	52	48	48	33
Mean			**26.6**	**13.9**	**2.1**	**6.6**	**67732**	**0.337**	**38.1**	**40.0**	**43.4**	**14.6**
STD			**1.8**	**4.3**	**2.2**	**3.6**	**47571**	**0.039**	**13.9**	**12.7**	**12.2**	**17.3**

Control: No parent with Alzheimer's disease and does not possess any copies of the APOE-ε4 allele; At-risk: Either one parent with Alzheimer's disease or one or two copies of the APOE-ε4 allele; MCI: clinically confirmed mild cognitive impairment (one ore more domain). MMSE: Mini-Mental State Exam (max score = 30); CERAD: Consortium to Establish a Registry for Alzheimer's Disease immediate (CERAD-I; max score = 30), delayed (CERAD-D; max score = 10) and recognition (CERAD-R; max score = 10) neuropsychological exam. Higher scores denote better performance on the exam. ICV: intracranial volume; CBF: cerebral blood flow; VBA: vertebrobasilar territory; RICA: right internal carotid artery territory; LICA: left internal carotid artery territory; STD: standard deviation.